Variation in performance of surfactant loading and resulting nitrate removal among four selected natural zeolites

Huade Guan [a,b,*], Erick Bestland [a], Chuanyu Zhu [a], Honglin Zhu [a], Dora Albertsdottir [a], John Hutson [a,b], Craig T. Simmons [a,b], Milena Ginic-Markovic [c], Xian Tao [d], Amanda V. Ellis [c]

[a] School of the Environment, Flinders University, Sturt Road, Bedford Park, SA 5042, Australia
[b] National Centre for Groundwater Research and Training, Flinders University, Sturt Road, Bedford Park, SA 5042, Australia
[c] Centre for NanoScale Science and Technology, School of Chemical and Physical Sciences, Flinders University, Sturt Road, Bedford Park, SA 5042, Australia
[d] Kimberley Global Pty Ltd, Adelaide, Australia

ARTICLE INFO

ABSTRACT

Surfactant modified zeolites (SMZs) have the capacity to target various types of water contaminants at relatively low cost and thus are being increasingly considered for use in improving water quality. It is important to know the surfactant loading performance of a zeolite before it is put into application. In this work we compare the loading capacity of a surfactant, hexadecyltrimethylammonium bromide (HDTMA-Br), onto four natural zeolites obtained from specific locations in the USA, Croatia, China, and Australia. The surfactant loading is examined using thermogravimetric analysis (TGA), Fourier transform infrared (FT-IR) spectroscopy, and Raman spectroscopy. We then compare the resulting SMZs performance in removing nitrate from water. Results show that TGA is useful to determine the HDTMA loading capacity on natural zeolites. It is also useful to distinguish between a HDTMA bi-layer and a HDTMA mono-layer on the SMZ surface, which has not been previously reported in the literature. TGA results infer that HDTMA (bi-layer) loading decreases in the order of US zeolite > Croatian zeolite > Chinese zeolite > Australian zeolite. This order of loading explains variation in performance of nitrate removal between the four SMZs. The SMZs remove 8–18 times more nitrate than the raw zeolites. SMZs prepared from the selected US and Croatian zeolites were more efficient in nitrate removal than the two zeolites commercially obtained from Australia and China.

© 2010 Elsevier B.V. All rights reserved.

1. Introduction

Zeolite is a collective term for a group of naturally occurring aluminosilicate minerals. The most abundant zeolitic mineral is clinoptilolite [1]. Clinoptilolite-rich zeolite has been widely used to improve water and air quality due to its large specific surface area and cation exchange capacity (CEC), low cost, and mechanical strength [1–4]. When placed in water raw zeolite particles have a net negative surface charge [5,6] and are hydrophilic which makes them inappropriate for the removal of anionic and hydrophobic pollutants. In order to improve the water contaminant remediation performance of zeolites, cationic surfactants have been successfully used to modify their surface properties [7–10].

One of the most commonly used surfactants for zeolite surface modification is hexadecyltrimethylammonium bromide (HDTMA-

Br or $C_{19}H_{42}N^+Br^-$) in which each molecule is composed of a hydrophilic and positively charged head group, and a hydrophobic tail. Depending on the coating conditions, HDTMA may form mono-layers or bi-layers on the zeolite surface [9]. The formation of a mono-layer occurs when the HDTMA's cationic head group attaches to the zeolite surface primarily via a cationic exchange process, that is, by replacing other exchangeable cations (such as Ca^{2+}, and K^+ [5]) present on the zeolite surface. When the HDTMA concentration in the feed solution is constantly kept above the critical micelle concentration (CMC, about 0.9 mM at 25 °C), a bi-layer results where the two layers of HDTMA are connected via hydrophobic affinity [10–12]. More often, a patchy mono-layer and/or bi-layers form on the surface [5,6]. With the loading of various surfactant compositions, the HDTMA modified zeolite (SMZ, hereafter) surface can have both hydrophilic and hydrophobic, as well as positively and negatively charged parts. In this manner SMZs can be used to target four major categories of contaminants, namely anions, cations, organics, and pathogens [7].

More recently there have been an increasing number of reports in the literature on the use of SMZs for the improvement of water

* Corresponding author at: School of the Environment, Flinders University, Sturt Rd., Bedford Park, Adelaide, SA 5042, Australia. Tel.: +61 8 82012319.
E-mail address: huade.guan@flinders.edu.au (H. Guan).

quality. The target contaminants include heavy metals [13–15], organic pollutants [16–19], organic dyes in waste water [20], nutrients [21], and microbial pathogens [22]. To widely apply the use of SMZs for water treatment, knowledge of the surfactant loading performance of selected zeolites is very important. Here we show a comparison in surfactant loading and nitrate removal performance of four selected naturally occurring zeolites and demonstrate a simple method using thermogravimetric analysis (TGA) to quickly determine the amount and structure of the loaded surfactant on the naturally occurring zeolites.

2. Materials and methods

2.1. Zeolite samples

Four zeolite samples, from specific locations in the USA, Croatia, Australia, and China were chosen for the study. The zeolite sample from the USA (SMZ-US hereafter) was previously pre-treated in the USA with HDTMA-Br and used as received from Prof. Bowman from New Mexico Tech, USA. The SMZ-US sample was prepared from a natural zeolitic tuff from the St. Cloud deposit near Winton, NM, USA with a clinoptilolite abundance of 74%. The sample has been reported to have a total CEC of 900 mequiv. kg^{-1} and an external cation exchange capacity (ECEC) of 100 mequiv. kg^{-1} [7]. The HDTMA surfactant loading and applications of the SMZ-US sample have been previously investigated [5,10–12,19,22–24] and provide a solid benchmark to examine the performance of the selected Croatian, Australian, and Chinese zeolites.

The zeolite sample from Croatia (Z-CR hereafter) had a clinoptilolite abundance of 60%, with a CEC of 1600 mequiv. kg^{-1} and an ECEC estimated at 160 mequiv. kg^{-1} [6]. This sample was provided by Dr. Hrenovic of University of Zagreb, Croatia.

Two other zeolite samples were obtained commercially. An Australian zeolite (Z-AU hereafter) was purchased from the Escott zeolite mine in Australia via Zeolite Australia Limited, consisting primarily of clinoptilolite with a CEC estimated at 1200 mequiv. kg^{-1}. The second zeolite was also a clinoptilolite-rich zeolite mined from Dushikou of Hebei Province China (Z-CN hereafter) and purchased from Beijing Panbao Limited. There were no CEC values provided with this sample.

2.2. Sample preparation and surfactant loading

Each of the three natural zeolite samples (Z-AU, Z-CR, and Z-CN) were sieved to obtain a particle size range between 1 and 2 mm. After being sieved they were washed with ultrapure (MilliQ) water (18.2 MΩ cm^{-1}) and dried in an oven at 105 °C for 24 h. The HDMTA-Br surfactant loading was then performed using the procedure previously described by Li and Bowman [5]. Typically, surfactant loading is performed at 25 °C [5,19] or 30 °C [6], after which the filtered SMZ is dried at room temperature. In order to speed up the drying process Schulze-Makuch et al. [22] dried their SMZ at 100 °C. In our work, due to the inherent insolubility of HDTMA-Br in water at room temperature, the feedstock (67 mM) was prepared at 45 °C. Loading of the surfactant was carried out by adding 180 g of each of the natural zeolite samples (Z-AU, Z-CR, and Z-CN) to 540 mL of the HDTMA-Br (67 mM) aqueous solution. The mixtures were then placed in a shaker water bath (60 strokes min^{-1}) for 24 h, with the temperature maintained at 45 °C. The zeolite/surfactant solution was then filtered through 0.45 μm filter paper, and the resulting SMZ was then rinsed three times with 400 mL of MilliQ water and finally air-dried at room temperature.

2.3. Mineralogical and surface characterization

Chemical compositions of the four zeolite samples were examined by a commercial lab (AcmeLabs, Canada), using LiBO$_2$/Li$_2$B$_4$O$_7$ fusion ICP-ES analysis. Z-AU, Z-CR, and Z-CN were examined in thin sections with a polarising microscope in order to determine the texture of the zeolite minerals with other minerals, and their intra-grain porosity.

Thermogravimetric analysis (TGA) was performed in order to quantify the amount of surfactant absorbed to the various zeolite surfaces. The samples were measured on an Auto TGA 2950HR V6.1A (TA Instruments, USA). They were heated from room temperature to 600 °C at a heating rate of 5 °C min^{-1} under a nitrogen flow rate of 50 mL min^{-1}. The temperature calibration was performed using standard alumel and nickel thermocouples. In order to reduce any physisorbed water on the zeolite surface, the samples were placed in a 105 °C oven for 24 h, and then placed in a desiccator prior to TGA analysis.

Fourier transform infrared (FT-IR) spectroscopy was used to obtain a spectral fingerprint of the organic component of the SMZ surface. Infrared spectra were collected on a Spectrum 400 FT-IR/FT-NIR Spectrometer (Perkin Elmer, USA). The SMZ-US and SMZ-CN samples were measured between 650–1800 and 2400–4000 cm^{-1}. Before analysis the SMZ samples were placed in an oven for 24 h at 105 °C in order to remove physisorbed water from the zeolite surfaces.

Raman spectroscopy was also used to characterize the organic components of the SMZ. Raman spectroscopy gives rise to specific vibrations corresponding to functional groups on the surface of the zeolite. Raman spectra were collected with a WiTEC *alpha300R* Microscope (Alphatech, New Zealand) in Raman mode using a 100× objective (numerical aperture 0.9) and a 532 nm (E_{laser} = 2.33 eV) laser operating at constant power for each experiment up to a possible maximum of ~60 mW. Raman data were collected by WiTEC Control software with the surface perpendicular to the excitation source and analysed in WiTEC Project software. Spectra were collected using an integration time of 1 s.

2.4. Nitrate removal experiments

To examine the performance of the resulting SMZs, nitrate sorption experiments were performed with four surfactant modified zeolites, i.e. SMZ-US, SMZ-CR, SMZ-AU, and SMZ-CN, and two raw zeolites (Z-CR and Z-CN) for comparison. Nitrate solution was prepared from KNO$_3$. For each sorption experiment, 5 g of each zeolite sample (SMZ or Z) was mixed with 100 mL of aqueous solutions of nitrate (0.10, 0.25, 0.50, 0.75, 1.00, 1.50, or 2.00 mM), and then placed in a shaker at 25 °C for 24 h. At the end of the 24-h period the solutions were filtered through 0.45 μm filter paper and analysed for nitrate with a μChem nutrient analyser (SYSTEA, Italy), with some samples measured with an Ion Chromatography ICS 1500 (Dionex, Canada). The difference in nitrate concentration before and after the experiment was used to calculate the amount of sorption nitrate. The pH of water may influence sorption processes abruptly if it changes the particle surface charge [25]. However, due to the fact that the SMZ has a large zeta-potential in water, within a normal pH range [5] the pH effect was not considered important and thus not monitored in the experiments.

3. Results and discussion

The chemical composition of the Z-US (based on the SMZ-US sample) and the other naturally occurring zeolites (Z-CR, Z-CN and Z-AU) are summarized in Table 1. Most of the zeolite samples have approximately the same composition however the Z-CR sample has

Table 1
Chemical composition of four zeolites (unit: weight percentage).

Composition	SiO$_2$	Al$_2$O$_3$	Fe$_2$O$_3$	MgO	CaO	Na$_2$O	K$_2$O	TiO$_2$	P$_2$O$_5$	MnO	LOI[b]	Sum
Z-US[a]	63.32	11.83	1.24	1.15	2.88	0.65	2.51	0.21	0.05	0.09	15.70	99.92
Z-CR	65.71	14.13	1.53	0.71	3.03	2.20	2.82	0.27	0.02	0.03	9.30	99.93
Z-CN	66.23	11.91	1.14	0.86	2.78	0.85	2.00	0.17	0.03	0.05	13.80	99.95
Z-AU	69.21	11.59	1.12	1.09	2.84	0.86	1.74	0.19	0.04	0.02	11.10	99.94

[a] This is based on the SMZ-US sample.
[b] LOI is loss of ignition.

a significantly higher Al$_2$O$_3$ and Na$_2$O content which may improve the cationic binding of the surfactant.

TGA provides information on the amount of energy required to remove surfactant molecules from the zeolite surface. This energy depends on whether the surfactant is present as a mono- or bi-layer on the zeolite surface. Thus, the temperatures at which particular mass losses occur can be related to surfactant structures on the zeolite surfaces. In addition, the mass loss during a specific temperature range provides estimates of the quantity of surfactant that is loaded on the zeolite samples. TGA results of the raw zeolite samples (not shown) show mass loss curves similar to those reported by Sullivan et al. [26]. Fig. 1(a–d) shows thermographs of SMZ-US, SMZ-CR, SMZ-CN and SMZ-AU, respectively. Mass loss below 200 °C is attributed to unbound and physisorb water. Between 200 and 300 °C the derivative curve peaks for SMZ-US (at 230 °C) and SMZ-CR (at 234 °C) (Fig. 1a and b) have been attributed to the unbound HDTMA from lower energy or less stabilized bonding sites on the zeolite surface when the HDTMA loading exceeds 50% of its ECEC [26]. Such lower energy bonding is most likely due to hydrophobic–hydrophobic interactions of interdigitated HDTMA and indicates the possibility of thickening of the surfactant layer beyond a mono-layer to either an admicelle-type structure or a bi-layer. The formation of this type of structure then gives rise to terminal free ammonium cations which act as nitrate ion binding sites.

Derivative-mass loss peaks around 230 °C were not observed for the SMZ-CN and SMZ-AU (Fig. 1c and d, respectively), indicating little formation of HDTMA surfactant bi-layers.

All SMZs show a mass loss derivative peak around 395 °C (Fig. 1) that is not previously reported. This higher temperature peak indicates a stronger bonding of the surfactant to the zeolite surface, and is most likely due to the electrostatic binding of the ammonium cation head group to the electronegative zeolite surface (the first layer hereafter). This first layer acts as a template for the hydrophobic–hydrophobic interdigitation of a second layer. The temperature required to break this type of bonding is weaker than an electrostatic interaction, and gives rise to the mass loss described previously between 200 and 300 °C [27].

Table 2 shows the calculated HDTMA loadings from the TGA data (in mmol kg^{-1}) for the first layer (between 300 and 475 °C) and the second layer (between 200 and 300 °C). For the first layer calculation, the molecular weight of HDTMA was used, while for the second layer, the molecular weight of HDTMA-Br is used. The SMZ-US sample has the highest loading overall (220 mmol kg^{-1}) and
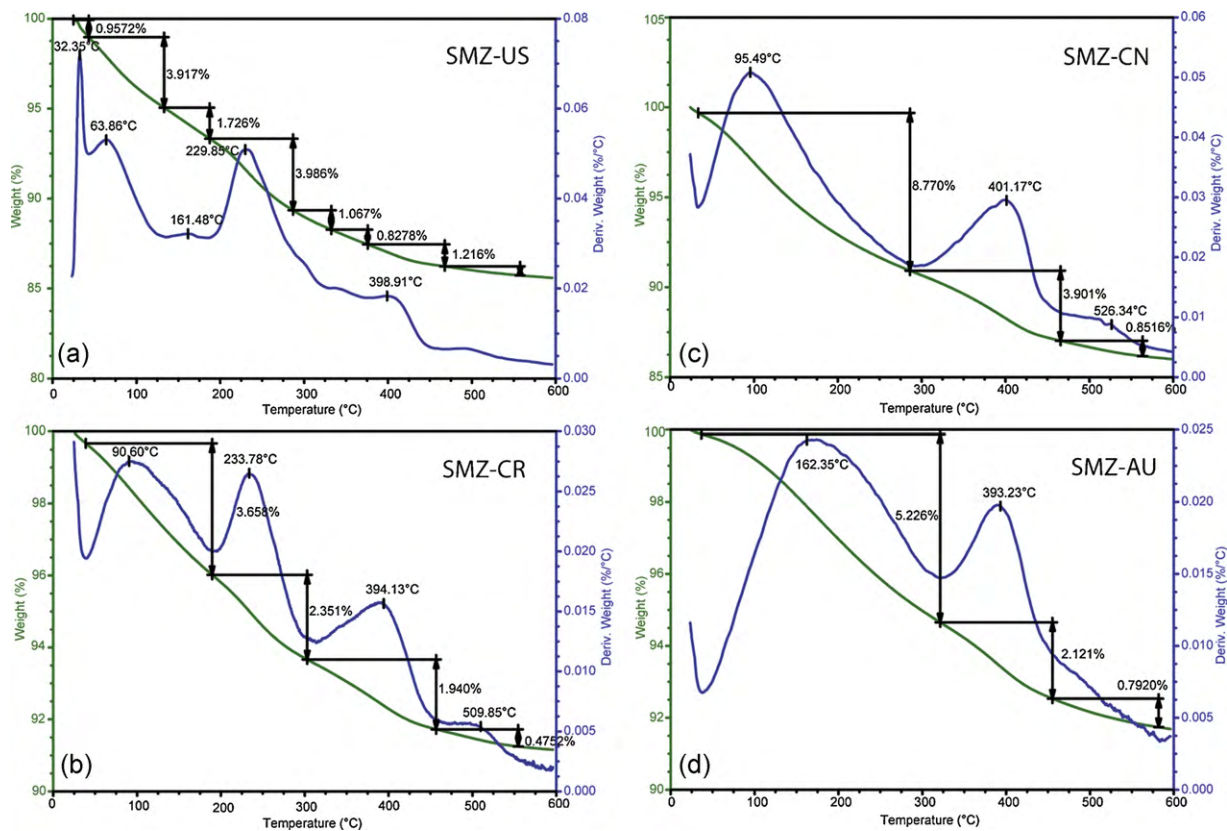
Fig. 1. TGA results of four HDTMA-Br-coated zeolites: (a) SMZ-US, (b) SMZ-CR, (c) SMZ-CN, and (d) SMZ-AU. The descending curve represents mass loss during the heating process (heating rate: 5 °C min^{-1}). The temperature marked on the derivative curve is the temperature around which the peak mass loss rate occurs.
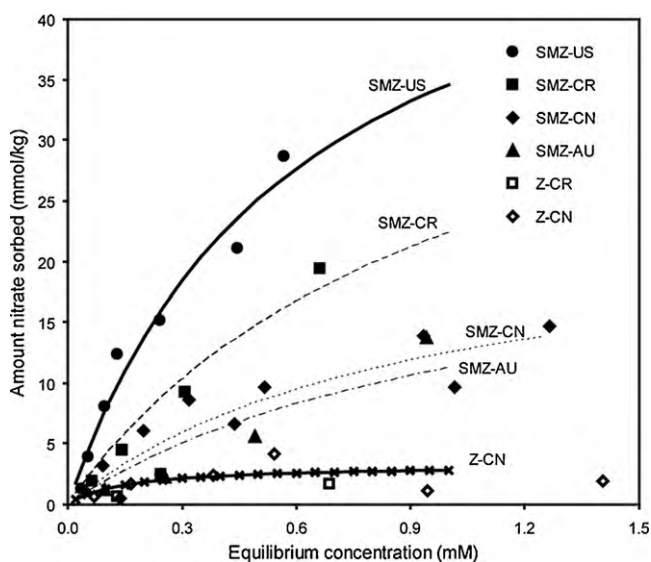
Table 2
Fitted Langmuir parameters for nitrate sorption on HDTMA-coated zeolites and one raw zeolite, and HDTMA loading of SMZs inferred from the TGA results (Fig. 2).

|	SMZ-US	SMZ-CR	SMZ-CN	SMZ-AU	Z-CN
Langmuir parameter					
S_m (mmol kg^{-1})[a]	56	45	24	24	3
K_L (L mmol^{-1})[a]	1.7	1.0	1.1	0.9	6.5
HDTMA loading (mmol kg^{-1})					
First layer	110	68	137	75	
Second layer	110	65	0	0	
Total loading	219	133	137	75	

[a] S_m represents the sorption maximum (or sorption capacity, mmol kg^{-1}) and K_L represents the Langmuir coefficient (L mmol^{-1}).

of both the first (110 mmol kg^{-1}) and the second (110 mmol kg^{-1}) layers. The total HDTMA loading of 220 mmol kg^{-1} is comparable to previous reports of 208 mmol kg^{-1} [11]. The first and second layer loading of SMZ-US is almost double that of SMZ-CR. The second layer loading is not inferred from the TGA data for SMZ-AU and SMZ-CN. The TGA-inferred HDTMA loading performance among the four SMZs is consistent with their performance in nitrate removal experiments that is discussed in the following.

Nitrate removal batch experiments were performed for all four SMZs and two raw zeolites (Z-CN and Z-AU). The results are summarized in Fig. 2. Table 2 shows fitted Langmuir parameters for nitrate sorption onto the SMZs and the Z-CN sample. The nitrate sorption capacity (S_m) of the Z-CN sample is 3 mmol kg^{-1}. After surface modification with HDTMA, nitrate ion removal is greatly enhanced to 24 mmol kg^{-1}. This is consistent with our understanding that the HDTMA double layer or the admicelle-type structure reverses the zeolite surface charges from negative to positive, facilitating electrostatic interactions between the nitrate ions and the SMZ particles. The order of S_m decreases in the following order SMZ-US (56 mmol kg^{-1}) > SMZ-CR (45 mmol kg^{-1}) > SMZ-CN (24 mmol kg^{-1}) = SMZ-AU (24 mmol kg^{-1}), with the raw zeolite Z-CN having the lowest nitrate removal performance (3 mmol kg^{-1}). This nitrate removal performance is clearly related to the amount and structure of the HDMTA loading. The improved performance of the SMZ-US is due to not only a higher HDTMA loading but also the second layer which has pendant ammonium head groups


Fig. 2. Isotherms for the adsorption of nitrate onto raw and HDTMA modified zeolites, resulted from the batch experiments performed in a shaker at 25 °C for 24 h. The lines are Langmuir model fits, with fitted parameters shown in Table 2. For the two raw zeolite samples, only Z-CN results are used for Langmuir isotherm fitting; the results of Z-CR are shown for comparison.
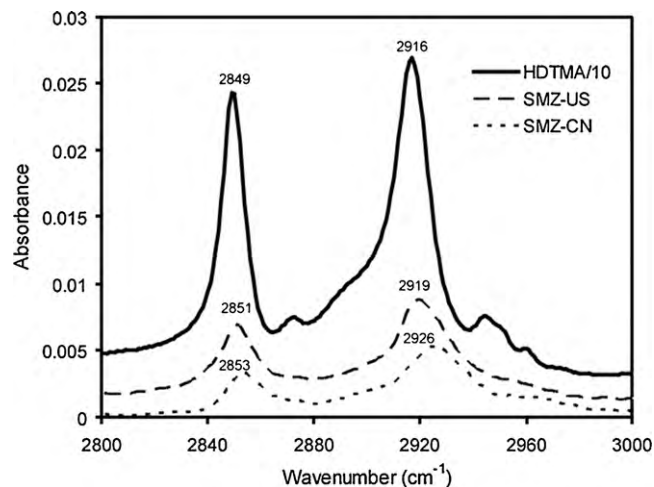

Fig. 3. FT-IR spectra of HDTMA (absorbance is divided by 10) and two selected HDTMA-Br-coated zeolites, SMZ-US and SMZ-CN.

for the extraction of nitrate from solution. In terms of surfactant modification the SMZ-CN and SMZ-AU samples showed the lowest nitrate removal efficiency and this was expected as there is no obvious second layer present on these samples. They do however have improved performance compared to raw zeolite (Z-CN) which may suggest some formation of patchy admicelle-type surfactant structures on the zeolite surfaces.

The conformation and environment of the HDMTA-Br surfactant and zeolite assembly was characterized by IR and Raman spectroscopy. Fig. 3 shows the high-frequency (2800–3000 cm^{-1}) region of the IR spectra of HDTMA-Br, SMZ-US and SMZ-CN, respectively. The HDTMA spectrum clearly shows the asymmetric and symmetric –CH$_2$ stretching modes of the hexadecyl chain at 2916 and 2849 cm^{-1}, respectively. Also present are the asymmetric and symmetric –CH$_3$ modes at 2960 and 2945 cm^{-1} which arise from the relative orientational freedom of the chain termini and typically an all-*trans* conformation. Differences arise in the IR spectra after the HDMTA cations have been loaded onto the zeolites. Peak shifts (δ) are used as a criterion for distinguishing changes in chemical environments of modes. Any δ value ≤ 2 cm^{-1} indicates no or little change in chemical environment. The SMZ-US spectra shows a moderate shift in both its asymmetric and symmetric –CH$_2$ stretching modes (Fig. 3) which corresponds to (2919 cm^{-1}, $\delta = +3$) and (2851 cm^{-1}, $\delta = +2$), respectively. These modes are essentially the same for the adsorbed and free HDTMA cations in solution, how-
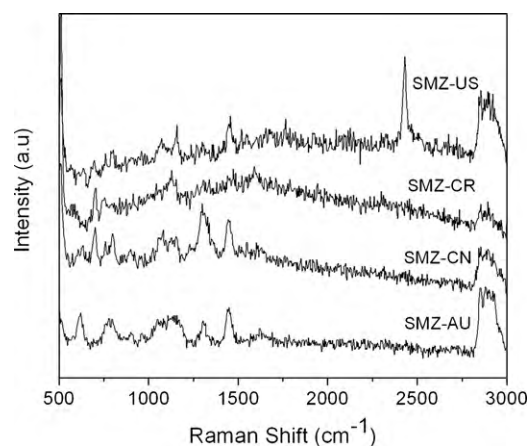
Fig. 4. Raman spectra of HDTMA-Br-coated zeolites, SMZ-US, SMZ-CR, SMZ-CN and SMZ-AU, with intensity values offset for clearer presentation.
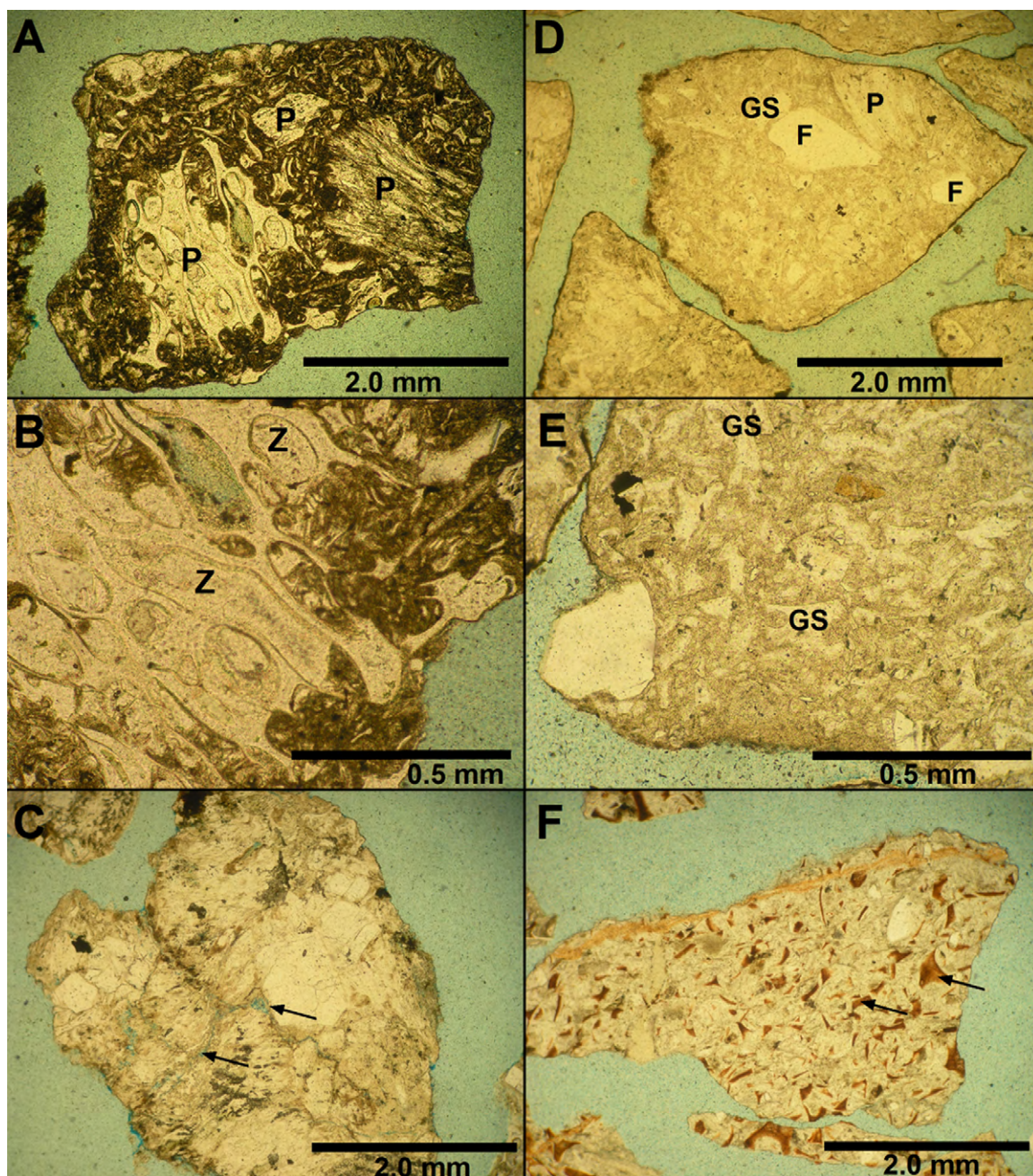
Fig. 5. Photomicrographs under plain polarising light of crushed zeolitic rocks from localities in Croatia (a–c), China (d, e), and Australia (f). Epoxy cement has been stained blue and fills pyroclastic bubble wall texture in the Croatian samples (a and b). P, pumice fragments; Z, blocky zeolite filling cement; GS, glass shard texture; F, feldspar. Arrows in (c) show cracks filled with epoxy cement. Arrows in (f) show glass shards that have been weathered to iron stained clay minerals.

ever, the moderately higher peak shift of the $-CH_2$ asymmetric mode indicates an increased gauche-like conformation and an indication of less ordered or structured tail (hexadecyl) groups than that of the free HDTMA in solution. Likewise, it could be indicative of an admicelle with less interfingering, slightly larger volume and some fragments of the tail group exhibiting varying trans/gauche changes [28]. This corresponds well with the data obtained for the nitrate removal (see Fig. 2) and TGA (see Fig. 1) where clearly the SMZ-US has improved nitrate removal performance due to excess cationic charge on the zeolite surface, while TGA shows the hydrophobic–hydrophobic binding release of interdigitated alkyl chains of an admicelle or bi-layer type structure. The SMZ-CN spectrum (Fig. 3) shows a more pronounced degree of disorder indicated by a shifting of both the asymmetric and the symmetric $-CH_2$

stretching modes to ($2926\,cm^{-1}$, $\delta = +10$) and ($2853\,cm^{-1}$, $\delta = +4$), respectively. The structure of the tail group is now far more disordered and it is unclear as to whether this is caused by a lower-, mid- or higher-coverage mono-layer on the zeolite surface Sullivan et al. [28]. From the nitrate removal data (see Fig. 1) the performance of this SMZ is clearly reduced presumably due to a lower availability of cationic charge.

Raman spectra of SMZ-AU, SMZ-CN, SMZ-CR and SMZ-US within the vibrational frequency range of $3000–500\,cm^{-1}$ are shown in Fig. 4. There appears clear evidence of organic groups present in all the samples observed as CH_2 stretching modes between 3000 and $2800\,cm^{-1}$, CH_2 bending modes between 1470 and $1400\,cm^{-1}$, and C–C stretching modes between 1200 and $1000\,cm^{-1}$. Within the vibrational region of $3000–2800\,cm^{-1}$ can also be found $CH_3–N^+$

symmetric stretch and CH_3-N^+ asymmetric stretch associated with the HDTMA ammonium head group. These are typically observed at a slightly higher frequency than the CH_2 stretching modes. Interestingly, it is the SMZ-US that appears to have one of the higher intensities in this region (Fig. 4). This implies that there are more free cationic head groups for the sorption of nitrate (also confirmed by the TGA and IR data). There also appears to be an additional sharp peak apparent in the SMZ-US spectrum but not in the others (Fig. 4) at $2434 \, cm^{-1}$. This is attributed to a tertiary amine salt (RNH^+), again proving that it is the SMZ-US sample which has the greater cationic charge available of all 4 surfactant modified zeolites studied. SMZ-CN and SMZ-AU show the highest intensities in the low frequency region ($1500–500 \, cm^{-1}$) mostly associated with the alkyl chain of the HDTMA. This indicates that the aliphatic chains are freely available on the surface of the zeolite and are therefore most likely present as a mono-layer or lower coverage mono-layer on the surface. This is corroborated by the low nitrate uptake of these samples (Fig. 2).

Raw zeolite Z-CR, Z-CN and Z-AU samples were examined in thin section with a polarising microscope in order to determine the texture of zeolite minerals with other minerals and intra-grain porosity (Fig. 5). All three samples examined have approximately the same grain size distribution and grain shape. The Z-CR sample has abundant pumice fragments and glass shards in an overall clayey matrix (Fig. 5a and b). The pumice fragments in this sample have standard pyroclastic "bubble wall texture" which has mostly been filled by blocky zeolite cement. Unfilled "bubble wall texture" or open pore space, now filled by blue epoxy cement, is common. This open "bubble wall texture", as well as cracks in the samples (Fig. 5c), represents significant intra-grain porosity. The Z-CN sample is dominated by glass shard texture with few "bubble walls" and does not display obvious intra-grain porosity (Fig. 5d and e), while the Z-AU sample is dominated by glass shard texture in which most of the glass shards have been altered to clay minerals (see arrows in Fig. 5f). The zeolite mineral in Z-AU sample occurs as secondary blocky veins and dispersed fine-grained zeolite between clay minerals. This sample also does not display obvious intra-grain porosity. These observations indicate that intra-grain porosity of the Z-CR sample may contribute to its better performance in surfactant loading and nitrate removal than the other two.

4. Conclusions

The adsorption behaviour of a quaternary ammonium cationic surfactant i.e. HDTMA (hexadecyltrimethylammonium) onto clinoptilolite-type zeolites has been investigated. SMZ samples prepared from four natural zeolites selected from US, Croatia, China, and Australia were investigated using TGA, FT-IR spectroscopy, Raman spectroscopy, and thin-section microscopy, and tested with nitrate removal experiments. Nitrate removal results of the SMZs suggest an 8–18 times higher removal capacity than raw zeolites. SMZs prepared from the selected US and Croatian zeolites are more efficient in nitrate removal than the two commercially obtained from Australia and China. The different SMZ nitrate removal performance can be explained by varying amounts of surfactant loading inferred from TGA where surfactant loading decreases in the order from the selected US zeolite, Croatian zeolite, Chinese zeolite, and to Australian zeolite. The hydrophobic interaction related to surfactant bi-layer loading is indicated as a mass loss peak in the TGA at approximately $230 \,°C$, while electrostatic binding related to mono-layer loading is shown as a peak at approximately $395 \,°C$. TGA-inferred HDTMA loading structures are corroborated by the analyses of FT-IR and Raman spectra. The thin-section results suggest that the zeolite samples with intra-grain porosity tend to undergo superior surfactant loading and thus subsequent nitrate removal.

References

[1] E. Erdem, N. Karapinar, R. Donat, The removal of heavy metal cations by natural zeolites, J. Colloid Interface Sci. 280 (2004) 309–314.
[2] M.W. Ackley, R.F. Giese, R.T. Yang, Clinoptilolite-untapped potential for kinetic gas separations, Zeolites 12 (1992) 780–788.
[3] Y.C. Chung, D.H. Son, D.H. Ahn, Nitrogen and organics removal from industrial wastewater using natural zeolite media, Water Sci. Technol. 42 (2000) 127–134.
[4] S. Kesraouiouki, C.R. Cheeseman, R. Perry, Natural zeolite utilization in pollution-control—a review of applications to metals effluents, J. Chem. Technol. Biotechnol. 59 (1994) 121–126.
[5] Z.H. Li, R.S. Bowman, Sorption of perchloroethylene by surfactant-modified zeolite as controlled by surfactant loading, Environ. Sci. Technol. 32 (1998) 2278–2282.
[6] M. Rozic, D.I. Sipusic, L. Sekovanic, S. Miljanic, L. Curkovic, J. Hrenovic, Sorption phenomena of modification of clinoptilolite tuffs by surfactant cations, J. Colloid Interface Sci. 331 (2009) 295–301.
[7] R.S. Bowman, Applications of surfactant-modified zeolites to environmental remediation, Microporous Mesoporous Mater. 61 (2003) 43–56.
[8] R.E. Apreutesei, C. Catrinescu, C. Teodosiu, Surfactant-modified natural zeolites for environmental applications in water purification, Environ. Eng. Manag. J. 7 (2008) 149–161.
[9] Z.H. Li, Sorption kinetics of hexadecyltrimethylammonium on natural clinoptilolite, Langmuir 15 (1999) 6438–6445.
[10] E.J. Sullivan, J.W. Carey, R.S. Bowman, Thermodynamics of cationic surfactant sorption onto natural clinoptilolite, J. Colloid Interface Sci. 206 (1998) 369–380.
[11] Z.H. Li, R.S. Bowman, Counterion effects on the sorption of cationic surfactant and chromate on natural clinoptilolite, Environ. Sci. Technol. 31 (1997) 2407–2412.
[12] Z.H. Li, S.J. Roy, Y.Q. Zou, R.S. Bowman, Long-term chemical and biological stability of surfactant modified zeolite, Environ. Sci. Technol. 32 (1998) 2628–2632.
[13] P. Chutia, S. Kato, T. Kojima, S. Satokawa, Adsorption of As(V) on surfactant-modified natural zeolites, J. Hazard. Mater. 162 (2009) 204–211.
[14] Z.H. Li, H.L. Hong, Retardation of chromate through packed columns of surfactant-modified zeolite, J. Hazard. Mater. 162 (2009) 1487–1493.
[15] S. Matijasevic, A. Dakovic, M. Tomasevic-Canovic, M. Stojanovic, D. Iles, Uranium(VI) adsorption on surfactant modified heulandite/clinoptilolite rich tuff, J. Serb. Chem. Soc. 71 (2006) 1323–1331.
[16] A. Kuleyin, Removal of phenol and 4-chlorophenol by surfactant-modified natural zeolite, J. Hazard. Mater. 144 (2007) 307–315.
[17] M. Sprynskyy, T. Ligor, M. Lebedynets, B. Buszewski, Kinetic and equilibrium studies of phenol adsorption by natural and modified forms of the clinoptilolite, J. Hazard. Mater. 169 (2009) 847–854.
[18] P.F. Zhang, D.M. Avudzega, R.S. Bowman, Removal of perchlorate from contaminated waters using surfactant-modified zeolite, J. Environ. Qual. 36 (2007) 1069–1075.
[19] J.M. Ranck, R.S. Bowman, J.L. Weeber, L.E. Katz, E.J. Sullivan, BTEX removal from produced water using surfactant-modified zeolite, J. Environ. Eng. ASCE 131 (2005) 434–442.
[20] O. Ozdemir, M. Turan, A.Z. Turan, A. Faki, A.B. Engin, Feasibility analysis of color removal from textile dyeing wastewater in a fixed-bed column system by surfactant-modified zeolite (SMZ), J. Hazard. Mater. 166 (2009) 647–654.
[21] J. Hrenovic, D. Tibljas, Y. Orhan, Increasing of the biomass of phosphate accumulating bacteria due to addition of a clinoptilolite-rich tuff from Bigadic, Turkey, in: Molecular Sieves: from Basic Research to Industrial Applications, Pts A and B, Elsevier Science Bv, Amsterdam, 2005, pp. 2089–2096.
[22] D. Schulze-Makuch, R.S. Bowman, S.D. Pillai, H. Guan, Field evaluation of the effectiveness of surfactant modified zeolite and iron-oxide-coated sand for removing viruses and bacteria from ground water, Ground Water Monit. Rem. 23 (2003) 68–74.
[23] Z. Li, Use of surfactant-modified zeolite as fertilizer carriers to control nitrate release, Microporous Mesoporous Mater. 61 (2003) 181–188.
[24] Z. Li, R. Beachner, Z. McManama, H. Hanlic, Sorption of arsenic by surfactant-modified zeolite and kaolinite, Microporous Mesoporous Mater. 105 (2007) 291–297.
[25] H. Guan, D. Schulze-Makuch, S. Schaffer, S.D. Pillai, The effect of critical pH on virus fate and transport in saturated porous medium, Ground Water 41 (2003) 701–708.
[26] E.J. Sullivan, D.B. Hunter, R.S. Bowman, Topological and thermal properties of surfactant-modified clinoptilolite studied by tapping-mode (TM) atomic force microscopy and high-resolution thermogravimetric analysis, Clay Clay Miner. 45 (1997) 42–53.
[27] B. Ha, K. Char, H.S. Jeon, Intercalation mechanism and interlayer structure of hexadecylamines in the confined space of layered alpha-zirconium phosphates, J. Phys. Chem. B 109 (2005) 24434–24440.
[28] E.J. Sullivan, D.B. Hunter, R.S. Bowman, Fourier transform Raman spectroscopy of sorbed HDTMA and the mechanism of chromate sorption to surfactant-modified clinoptilolite, Environ. Sci. Technol. 32 (1998) 1948–1955.